ELSEVIER

Journal of Chromatography A, 809 (1998) 159–171

JOURNAL OF CHROMATOGRAPHY A

# Salt effects in capillary zone electrophoresis II. Mechanisms of electrophoretic mobility modification due to Joule heating at high buffer concentrations

Reginald F. Cross*, Jing Cao

*School of Engineering and Science, Swinburne University of Technology, John Street, Hawthorn, Victoria 3122, Australia*

Received 10 October 1996; received in revised form 26 February 1998; accepted 27 February 1998

**Abstract**

Five sulphonamides spanning a range of initial degrees of ionisation have been used as probes for the study of the mechanisms of electrophoretic mobility modification caused by increasing buffer concentrations (5–210 m*M* sodium phosphate) in capillary zone electrophoresis (CZE). Partition experiments at the CZE operational pH and a second pH where the analytes are uncharged permits independent determinations of the salt and temperature effects upon ionisation. At the CZE temperature, the underlying salt effects due to nonideal solute–solvent interactions are demonstrated. These are selective and indicate that the buffer concentration may be manipulated to facilitate resolution of analytes with differing degrees of ionisation. These selectivities are heightened by Joule heating. At elevated temperatures, the relative effects upon ionisation and viscosity were determined. These magnitudes were then combined and used in conjunction with the deviations in electrophoretic mobilities from the extrapolated behaviour of dilute buffers to estimate mean internal capillary temperatures. 

*Keywords:* Salt effects; Electrophoretic mobility; Buffer composition; Joule heating; Sulphonamides

## 1. Introduction

Joule heating in capillary zone electrophoresis (CZE) is the by-product of the electrical work done in passing a current through the resistive buffer solution in the capillary. As a result, the internal temperature is raised, the viscosity decreases and the solutes' diffusion coefficients increase [1]. In the case of the buffer ions that form the excess charge on the solution side of the electrical double layer at the walls of the silica capillary, an increase in mobilities leads to increased electroosmotic flow (EOF). And in the case of the analytes, electrophoretic mobilities ($\mu_{ep}$) are significantly affected [2].

The generated heat is dissipated radially by conduction along three distance intervals: from the centre of the capillary to the wall, across the capillary wall and from the wall to the surrounding air. This can create a parabolic temperature gradient from the centre to the wall of the capillary and a parabolic diffusional profile which results in axial band-broadening. In extreme cases this 'thermal mixing' can lead to peak loss [2–6].

Early estimates of the effect of Joule heating on the number of theoretical plates attainable under the range of conditions commonly used in the practice of

*Corresponding author.

0021-9673/98/$19.00 
PII: S0021-9673(98)00189-7

CE were encouraging. Knox [7] calculated the boundary conditions under which the plate height contribution from thermal effects was considered negligible compared to the plate height contribution from axial diffusion and concluded that there should not be any significant band-broadening in the usual practice of CE. Also, Grushka et al. [8] provided the maximal allowable capillary diameters under several circumstances. For example, their calculations indicated that no negligible loss in the height equivalent to a theoretical plate (HETP) will occur for capillaries between 50 and 100 μm internal diameter with 30 kV $m^{-1}$ applied for small molecules in 0.1 *M* buffers.

It appears that these conclusions were incorrect. Knox and McCormack [1] have since stated that: 'It is obvious from previously published work (any typical CE application) and results to be presented here that their treatment overlooked a major source of band broadening.' That source was the change in viscosity and rates of diffusion. Lui et al. [9] used laser Raman thermometry to determine internal capillary temperatures and radial profiles. Their data indicates significant Joule heating. For a field strength of 300 V/cm applied along a 75 μm I.D.× 205 μm O.D. fused-silica capillary filled with 25 m*M* phosphate buffer (pH 7.4) and with forced air cooling, the average internal temperature rose 18°C from the ambient temperature of 22°C. The profile across the radius of the capillary was flat but contained a drop of the order of 1°C from the centre to the internal wall of the capillary. These experimental conditions are not atypical of those commonly used and indicate increased band-broadening due to longitudinal diffusion rather than due to a distorted radial flow profile. Furthermore, Yu et al. [10] have found increased dispersion in micellar electrokinetic chromatography (MEKC) at higher field strengths which they suggest may be due to Joule heating.

However, between the onset of Joule heating (as evidenced by changes in the electroosmotic and electrophoretic mobilities) and the catastrophic effects of excessive heat production, there is a range of experimental conditions under which the increased time of analysis should generally lead to enhanced resolution. One such set of circumstances is provided by higher buffer concentrations. Janini and co-workers have demonstrated the existence of this window of enhanced resolution for dansyl amino acids in acetate and phosphate buffers [11,12]. Also, we have observed the gradual separation of two dihydrofolate reductase inhibitors of almost identical charge to volume ratio with increasing salt concentration without significant deterioration of the electropherograms due to increased band-broadening [13,14]. Thus CZE in high buffer concentrations holds considerable promise for difficult separations. However, the use of high buffer salt concentrations will lead to other changes in solution. These include potential alterations to the degree of ionisation of weak acids and bases (which may vary from analyte to analyte and provide an additional source of selectivity) and the universal effect upon $\mu_{ep}$ for all analytes due to Joule heating; increased temperature and decreased viscosity. The increased temperature will also affect water and buffer ionisation equilibria.

It is therefore of fundamental importance that these effects are understood and that the relative magnitudes are established. It is also useful to know the mechanisms by which analyte mobilities may be manipulated in order to facilitate separations.

In this investigation of ionisation and thermal effects, the variation of electrophoretic mobilities is examined as a function of buffer concentration over a wide range and individual causes of deviation from dilute solution behaviour are isolated. Five sulphonamides with significant but widely varying degrees of ionisation have been chosen as the analytes (in sodium phosphate buffers).

## 2. Theory

In the pH region of experimentation, the chosen sulphonamides are all deprotonated and ionised at the amide nitrogen, to some extent (Eq. (1)):

$$SFA - H_{aq} + H_2O \rightleftarrows H_3O^+ + SFA^- \quad (1)$$

and the degree of ionisation ($\alpha$) is given by:

$$\alpha = \frac{[SFA^-]}{[SFA^-] + [SFA - H]_{aq}} \quad (2)$$

If $c_{aq}$ is the total (or analytical) concentration of

the sulphonamide in the aqueous phase, Eq. (2) becomes:

$$\alpha = \frac{c_{aq} - [SFA - H]_{aq}}{c_{aq}} \quad (3)$$

When equilibrated with an immiscible organic solvent, partitioning will occur according to Eq. (4):

$$SFA - H_{aq} \rightleftarrows SFA - H_{org} \quad (4)$$

and the concentration (′) partition constant $P'$ will be given by Eq. (5):

$$P' = \frac{[SFA - H]_{org}}{[SFA - H]_{aq}} \quad (5)$$

Rearrangement of Eq. (5) and substitution for $[SFA-H]_{aq}$ into Eq. (3) yields:

$$\alpha = \frac{c_{aq} - [SFA - H]_{org}/P'}{c_{aq}} \quad (6)$$

Eq. (6) provides a ready mechanism for the determination of $\alpha$. $P'$ is determined unambiguously by measurements of $[SFA-H]$ in both phases at pH 5 where there is no significant ionisation[1].

With a value of $P'$, $c_{aq}$ is calculated at the pH of interest (7) from a direct measurement of $[SFA-H]_{org}$ and mass balance over the two phases.

## 3. Experimental

### 3.1. Instrumental

A Model 270A CE system by Applied Biosystems (Foster City, CA, USA) was used for all CZE experiments. The analytes were detected by UV absorbance at 254 nm and the detector time constant was set at 0.3 s in all experiments.

The determinations were performed on a 67.3 cm×50 μm I.D. (220 μm O.D.) fused-silica capillary (Applied Biosystems) with the detection window located 49 cm from the injection end. Vacuum injection took place at the anode (+) and all experiments were performed at the thermostatted temperature of 30°C. Electropherograms were recorded on a DeskJet Plus recorder and data were collected and integrated with a Model 270 CE system interfaced to an Apple Macintosh computer.

A Cary model 13E UV–vis spectrophotometer system by Varian (Mulgrave, Australia) was used for the determination of degrees of dissociation. The analytes were detected by UV absorbance at 264 (SMZ) or 280 nm (ST).

### 3.2. Chemicals and materials

The five sulphonamides (SFA) [sulphamethazine (SMZ), sulphathiazole (ST), sulphamethizole (SMI), succinyl sulphathiazole (SST) and phthalyl sulphacetamide (PSAC)] used in the study were obtained from Sigma (St. Louis, MO, USA). The structures and p$K_a$ values of the above compounds are shown in Table 1.

For the CZE experiments, standard stock solutions of each compound were prepared by dissolving 0.1 g in 100 ml of HPLC grade methanol (BDH). Each compound was diluted with Milli-q water to give a final concentration of 25 ng/μl. Sample solutions were filtered (0.45 μm) before injection. Sodium phosphate buffers at 5–210 m$M$ with respect to phosphate were prepared using $Na_2HPO_4$ and $NaH_2PO_4$. Where necessary, solutions were adjusted

[1] It has long been known that the partition behaviour of the sulphonamides between aqueous phases and any specific nonpolar medium is solely determined by the degree of ionisation in the aqueous phase, which is primarily determined by pH, but will also be affected by ionic strength, the type of buffer utilised, etc. For the majority of sulphonamides, there is an anilinium group for which p$K_{a,1}$ is around 2–2.5 (see Table 1). p$K_{a,2}$ applies to the ionisation of the sulphonamide nitrogen (Eq. (1)) and lies between 7 and 7.5 for SMZ and ST, the two analytes to be examined with respect to ionisation. Hence, ionisation should be negligible around pH 5 for these two sulphonamides and there appear not to be any factors other than these known ionisations that cause variations in partitioning processes. For sulphamethoxydiazine the variation of the apparent partition constant with pH is as predicted on the basis of the p$K_a$ data [15]. And for the other sulphonamide for which there are multiple values of the partition constant measured in the same solvent but at different pH values (sulphathiazole), correction for ionisation gives an approximately constant value [15]. The final indication of the absence of factors other than these known ionisations causing variations in partitioning processes comes from a study of the retention of sulphonamides on nonpolar porous copolymers using HPLC [16]. Over the pH range of 1–13, the experimentally determined retention ($k'$) is exactly replicated by calculated values based on the p$K_a$ values for seven sulphonamides.

Table 1

**General structure:**

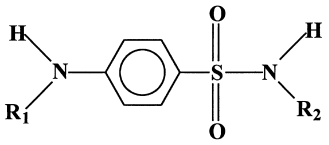

| SFA | Structure | | $pK_{a,1}$ | $pK_{a,2}$ |
|---|---|---|---|---|
| SMZ | $R_1$: H | $R_2$: 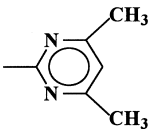 | 2.4 | 7.4 |
| ST | $R_1$: H | $R_2$: 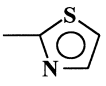 | ---- | 7.2 |
| SMI | $R_1$: H | $R_2$: 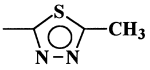 | ---- | 5.4 |
| SST | $R_1$: 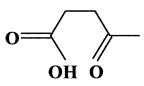 | $R_2$: 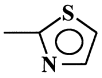 | 4.16 (Ca.) | 7.2 (Ca.) |
| PSAC | $R_1$: 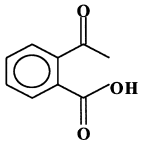 | $R_2$: 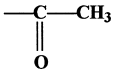 | 2.89 (Ca.) | 5.4 (Ca.) |

to exactly pH 7 with 20% $H_3PO_4$ or 0.1 *M* NaOH. All chemicals were of analytical-reagent grade and Milli-Q water was used to prepare all solutions.

Organic extractions were performed with ethyl acetate–chloroform (1:1, v/v) mixtures.

### *3.3. Methods*

#### *3.3.1. CZE*

Capillary preparation at the start of each day of experimentation involved initial purging with 0.1 *M* NaOH for 3 min, followed by Milli-Q water purging for 3 min and then the running buffer for 3 min. Between runs, the capillary was purged with 0.1 *M* NaOH for 3 min followed by running buffer for 3 min. Vacuum injections of 7-s duration were used. At the nominal 4 nl/s [17], 28 nl would have been injected. However, the more viscous buffers used would lead to greatly reduced injection volumes. Furthermore, as the sample was dissolved in water,

sample stacking compensated for this larger than usual volume.

The methanol in the sample solvent acted as a neutral marker (NM) by causing a baseline disturbance in the electropherograms and providing a measure of $t_{NM}$. The electrophoretic mobility ($\mu_{ep}$) was then calculated as usual:

$$\mu_{ep} = \frac{L_D L}{V}\left(\frac{1}{t_{NM}} - \frac{1}{t_m}\right)$$

$V$ is the applied voltage, $L$ is the length of the capillary, $L_D$ the length to the detector and $t_m$ is the apparent migration time of the analyte.

### *3.3.2. Determination of partition constants and degrees of ionisation*

SMZ and ST standards were prepared by direct dissolution of the solids into the aqueous buffer and the ethyl acetate–chloroform (50:50, v/v) solvent. Parallel dilutions of these stock solutions in their solvents were used to determine UV absorbances and the standard curves had correlation coefficients (seven points) of 0.9999 for ST in both phases and 1.0000 for SMZ.

Equal volumes (5 ml) of aqueous buffer and organic solvent were used in all extractions and the partitioning systems were thermostatted in a water-bath at the temperatures stated in Section 4. The phases were vigorously shaken every 10 min and constancy of the UV absorbance indicated that equilibrium was reached after 30 min. The aqueous buffer was removed by vacuum pipette before sampling.

For the determination of the partition constants, approximately 0.0010 g of SMZ or ST was dissolved in the pH 5 phosphate buffers (at the same ionic strength as the pH 7 phosphate buffers) and the UV readings recorded. By reference to the standard curves the exact concentrations of the SFA were determined. After partitioning, the UV absorbances in the organic solutions were measured, the SFA concentrations determined from the organic phase standard curves and $c_{aq}$ calculated from mass balance.

Determination of the degrees of ionisation were done using the above procedures with the CZE phosphate buffers at pH 7.

## 4. Results and discussion

As the a major aim of this investigation was to determine the relative magnitudes of ionisation and $\mu_{ep}$ changes due to salt effects in the presence (and absence) of Joule heating, it was necessary to operate under conditions of high power output to ensure Joule heating. Additionally, since the effect of increasing the ionic strength of the buffer is primarily to extend the analysis time [11,12], it is imperative to work with large driving voltages to ensure that the advantages of the high salt concentrations can be utilised without sacrificing the practicality of minimal run times. Thus the first experiments involved taking the highest buffer concentrations allowed by solubility and specifically testing these with increasing voltages to see how high it was possible to go without adverse effects. The undesirable effects were loss of current (instrumental shutdown), peak loss, excessive noise (as observed in the separation of the dihydrofolate reductase inhibitors in 250 m*M* sodium phosphate buffers [13]) or peak-broadening sufficient to lead to loss of resolution relative to lower buffer concentrations [11]. When deterioration was observed (generally instrument shutdown or excessive noise), the applied potential was reduced by a few kV for good measure. Hence analysis times were as short as possible. We consider this to be the optimum practical driving voltage (OPDV).

### *4.1. Joule heating*

Linear plots of the migration times of dansyl amino acids versus the square root of concentration have been obtained by Issaq et al. for buffers in the 25 to 75 m*M* range [11]. For acetate buffers the applied field was 90 V cm$^{-1}$ and for phosphate buffers 360 V cm$^{-1}$. In these cases, the effect of Joule heating on electrophoresis can apparently be neglected because of the low buffer concentrations. To examine the influence of Joule heating, sodium phosphate concentrations from 5 to 210 m*M* were examined at 18 kV (267.5 V cm$^{-1}$). Fig. 1 shows the migration times of the SFA to be approximately linear versus the square root of the buffer concentration in the range from 5 to 35 m*M* ($c^{1/2} \approx 2$–6). At higher concentrations the plots start to curve up. This deviation is presumed to be caused by Joule

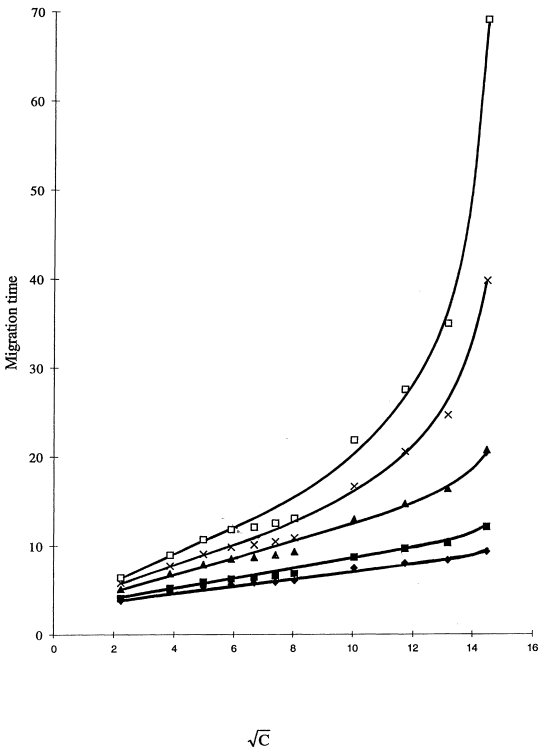


Fig. 1. Migration times (min) of the SFA versus the square root of the sodium phosphate buffer concentration (m*M*), with 18 kV applied at pH 7. Legend: (♦) SMZ, (■) ST, (▲) SMI, (×) SST, (□) PSAC.

heating. However, Table 2 provides independent support for the presence of Joule heating. In the highest buffer concentrations used in this study (210 m*M*), electroosmotic mobilities were measured at seven applied voltages up to the 18 kV used to obtain the data in Fig. 1. It is observed in Table 2 that the electroosmotic mobilities increase with rising voltage. Furthermore, plots of the electrophoretic mobilities of the SFA versus the reciprocal square root of ionic strength of the buffer (Fig. 2) also show deviations from the linear dependence expected at low salt concentrations [11].

Table 2
Variation in electroosmotic mobilities, $\mu_{eo}$ ($\cdot 10^{-5}$ cm$^2$ V$^{-1}$ s$^{-1}$) with applied voltage

| Voltage (kV) | $\mu_{eo}$ |
|---|---|
| 6.0 | 26.54 |
| 8.0 | 29.17 |
| 10.0 | 30.61 |
| 12.0 | 32.63 |
| 14.0 | 35.32 |
| 16.0 | 39.87 |
| 18.0 | 44.46 |

In Fig. 1, in the range $\sqrt{C}=6$–8 the experimental data appears to oscillate significantly from the lines of best fit drawn to each data set overall. This is the same deviation that may be seen in Fig. 2 for $1/\sqrt{I}=3$–5. During the course of review, the nature of this oscillation was questioned. It is at least partly a reflection of the variation in the electroosmotic mobility ($\mu_{eo}$) with buffer concentration. That is, a plot of $\mu_{eo}$ versus $1/\sqrt{I}$ shows an upward deviation from the curve of best fit over the same range of buffer concentrations. Although a consistent conditioning procedure was practised (see Section 3.3), some difference in the state of the capillary is implied. As we have found the repetition of parts of

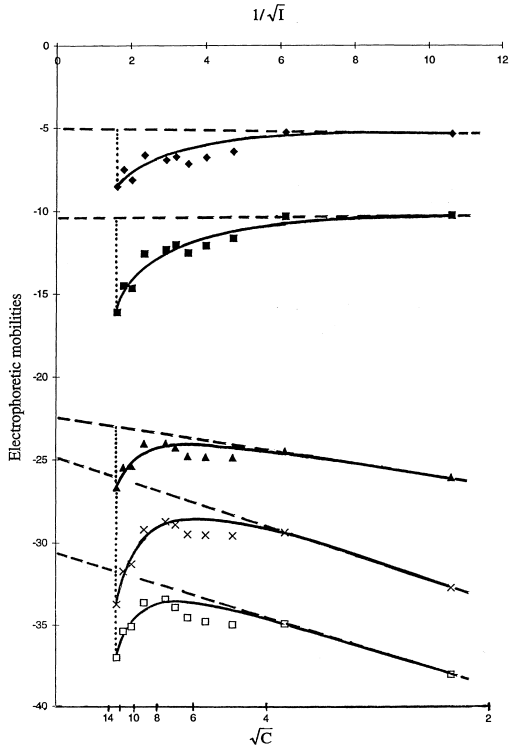


Fig. 2. Electrophoretic mobilities of five SFA (cm$^2$/$10^{-5}$ V s) versus the reciprocal of the square root of ionic strength of the sodium phosphate buffer. (The lower abscissa scale is the same as for Fig. 1). Legend for the compounds as in Fig. 1. The dots are the experimental points, the solid lines the lines of best fit and the dashed lines the extrapolation of the observed behaviour in dilute buffers.

a sequence of measurements unhelpful on other occasions — whether it be just $\mu_{eo}$ or $\mu_{ep}$ as well, we did not attempt to remeasure selected mobilities in the range of buffer concentrations in question. Again, difficulty with reproducibility appears to be related to capillary age and condition. We did repeat the entire data set, but with an expanded number of analytes and buffer concentrations. This showed that the relative positions of the $\mu_{ep}$ versus $1/\sqrt{I}$ plots (for the five analytes used in this study) were maintained and the plots were located in approximately the same place relative to the $\mu_{ep}$ axis. Furthermore, the shapes of the plots and the relative changes of $\mu_{ep}$ versus $1/\sqrt{I}$ with increasing buffer concentration for the various analytes were generally the same. Unfortunately, the plot of $\mu_{eo}$ versus $1/\sqrt{I}$ again contained some irregularities (although at different buffer concentrations) and the scatter in the $\mu_{ep}$ data was greater. Hence the second set of data confirmed the set shown in this paper, but displayed greater experimental error, presumably again due to conditioning and ageing problems. However, it is quite clear that the apparently systematic oscillation observed in Figs. 1 and 2 was not reproduced and must be presumed to be an artefact.

### *4.2. Salt and temperature effects upon ionisation*

Whilst the evidence for Joule heating seems clear, for the variation in electrophoretic mobilities as a function of buffer concentration (Fig. 2), the question arises as to whether there is a concurrent contribution to the observed deviations from expected behaviour due to the underlying variation in ionic strength ($I$). Salt effects upon chemical equilibria are well known and are derived from changes in the activity coefficients ($\gamma$) and therefore chemical potentials ($\mu$) of the reagents and products. Whilst possibly inconsequential at the lower buffer concentrations generally used in CZE, the effects of solute nonideality cannot be presumed to be negligible at higher values of $I$.

In the case of the electrophoretic mobilities, it is equilibrium 1 and the degree of ionisation that may vary. Ionic species universally experience decreased activity coefficients ($\gamma_{\pm}$) and chemical potentials ($\mu_{\pm}$) over the range of $I$ used to obtain the data in Fig. 2 [18]. This includes organic ions [19]. Thus, via this mechanism the $SFA^-$ will be thermodynamically stabilised with respect to SFH–H and increased ionisation is expected. On the other hand, this assumes that $\gamma(SFA-H)$ is unaffected by changes in $I$. This is unlikely. The activity coefficients of nonelectrolytes are generally subject to salt effects. However, the sign and magnitude of the effects are less predictable. Nonelectrolytes generally 'salt out'. That is, $\gamma$ and $\mu$ usually increase and the solubility decreases. This would reinforce the tendency to enhanced ionisation caused by the salt effect on the charged conjugate. Small and polar molecules are less strongly salted out, and salting out is weaker in salts with larger anions like nitrates and perchlorates [20,21]. Indeed, methyl acetate 'salts in' in sodium perchlorate solutions and is an exception [21]; $\gamma$ and $\mu$ decrease. The SFA are bigger molecules, but they also contain a larger number of more polar segments. Thus, in an electrolyte with a larger anion such as phosphate, the salt effect might be expected to be small, but would be of uncertain sign. Hence, the net effect of $I$ upon the equilibrium positions of the dissociation reactions of the SFA are difficult to predict, although increased ionisation and mobility seem the most likely.

Table 3 shows the values of $P'$ measured at pH 5 for SMZ and ST. Within experimental error, it is clear that the salt effect upon $P'$ is minimal but the temperature effect is significant.

Table 4 gives the values of $\alpha$ calculated from Eq. (6), $P'$ and the partition experiments at pH 7. As with $P'$, measurements have only been carried out on two of the five analytes (SMZ and ST). With a $pK_{a,2}$ of 5.4, SMI will be almost 98% ionised at pH 7 and will therefore be incapable of a significant increase in ionisation, either due to the increasing ionic strength of the buffer or Joule heating. Furthermore, changes in ionisation within 1–2% would probably be inside the experimental error of the method of determination used. The same applies to PSAC. Although a $pK_{a,2}$ value for PSAC is not known, it cannot be appreciably different to that of sulphacetamide (5.4). Similarly, $pK_{a,2}$ for SST must be almost identical to that for ST and it has been assumed that changes in ionisation will be similar under the same circumstances.

The values of $\alpha$ in Table 4 clearly indicate changes in ionisation due to changing buffer concentration. At every temperature the degree of ioni-

Table 3
Values of the concentration partition constant ($P'$) as a function of phosphate concentration and temperature

| Sulfonamide | Temperature (°C) | $P'$ | | | |
|---|---|---|---|---|---|
| | | Buffer concentration | | | |
| | | 101 m*M* | 138 m*M* | 174 m*M* | 210 m*M* |
| SMZ | 30 | 6.45 | 6.30 | 6.44 | 7.01 |
| | 40 | 5.17 | 5.46 | 6.19 | 5.58 |
| | 50 | 4.42 | 4.58 | 4.61 | 4.79 |
| | 60 | 3.89 | 4.08 | 4.33 | 4.65 |
| ST | 30 | 0.767 | 0.872 | 0.864 | 0.811 |
| | 40 | 0.671 | 0.673 | 0.708 | 0.715 |
| | 50 | 0.622 | 0.586 | 0.591 | 0.599 |
| | 60 | 0.565 | 0.530 | 0.555 | 0.568 |

sation increases for SMZ and decreases for ST. In terms of the nonideal behaviour of the solutes in response to increasing $I$, it is variations in the $\gamma$(SFA−H) that are consistent with the structural differences of the electrically neutral analytes, that are clearly implied. In the case of the smaller and more polar ST, salting in — or stabilisation of the electrically neutral conjugate acid via a decreased $\gamma$ — to a greater extent than that experienced by the charged conjugate base ($SFA^-$) is inferred. On the other hand, for the larger and less polar molecular form of SMZ there is a smaller decrease in the chemical potential than there is for the anion.

This 'salt effect' is discriminatory. Some analytes are affected and some are not. Highly ionised salts cannot be greatly affected but weakly ionised analytes are subject to significant percentage changes in ionisation and therefore mobility. Thus selectivities and hence resolution may also be significantly changed by increasing the concentration of the buffer. This provides an alternative method for the manipulation of relative mobilities and would be invaluable where the benefits of a higher pH due to increased ionisation and electrophoretic mobility could be nullified (or worse) by even larger increases in the EOF (for analytes migrating in the opposite direction to the EOF).

Over the ranges examined, the temperature effects on the ionisation equilibria for both SMZ and ST at all buffer concentrations were larger than the isothermal salt effects. The magnitude of the temperature effect is not strongly dependent upon the buffer concentration and is similar for the two analytes, albeit somewhat larger for SMZ than ST, on average.

Because the ionisation of the weakly ionised analytes are enhanced by increasing temperature,

Table 4
Degree of ionisation ($\alpha$) of sulphonamides in phosphate buffers

| Sulphonamide | Temperature (°C) | $\alpha$ | | | |
|---|---|---|---|---|---|
| | | Buffer concentration (m*M*) | | | |
| | | 101 | 138 | 174 | 210 |
| SMZ | 30 | 0.328 | 0.339 | 0.388 | 0.423 |
| | 40 | 0.386 | 0.465 | 0.425 | 0.461 |
| | 50 | 0.436 | 0.489 | 0.497 | 0.521 |
| | 60 | 0.627 | 0.627 | 0.631 | 0.656 |
| ST | 30 | 0.400 | 0.409 | 0.397 | 0.328 |
| | 40 | 0.433 | 0.427 | 0.411 | 0.389 |
| | 50 | 0.501 | 0.455 | 0.421 | 0.436 |
| | 60 | 0.566 | 0.525 | 0.518 | 0.464 |

increases in temperature therefore heighten the selectivity changes available from increasing buffer concentrations. Thus Joule heating can be an aid to the resolution of difficult-to-separate analytes. If greater advantage was needed to be taken of the temperature dependence of selective ionisation changes, the oven temperature could be increased. Should Joule heating then become a problem, it would be appropriate to decrease the voltage a little and keep the analysis time within reasonable bounds.

### *4.3. Relative effects of temperature upon the electrophoretic mobility via decreased viscosity and increased ionisation*

The electrophoretic mobility, $\mu_{ep}$, is usually given by Eq. (7):

$$\mu_{ep} = \frac{Z}{6\pi\eta r} \tag{7}$$

However, we have recently [22] found strong evidence to support a more complex relationship between $\mu_{ep}$ and the usual variables:

$$\mu_{ep} = \frac{Z}{6\pi\eta r^2} \cdot \frac{1}{3.30 \cdot 10^7 \sqrt{I}} \tag{8}$$

Eq. (8) indicates that a plot of $\mu_{ep}$ versus $1/\sqrt{I}$ will be linear for any migrating analyte, provided that the temperature and ionisation remain constant and the Debye–Hückel limiting law is valid. For a particular ion ($r$ fixed), both Eqs. (7) and (8) indicate that there will be two mechanisms of modification at elevated temperatures ($T$). Both the charge ($Z$) (which is equal to the degree of dissociation ($\alpha$) for SMZ and ST) and the viscosity ($\eta$) may change. Fig. 3 shows the relative change in $1/\eta$, $[(1/\eta_t)/(1/\eta_{30})]$, and the relative changes in ionisation for SMZ and ST, $[\alpha(t,I)/\alpha(30,I)]$, plotted as a function of temperature. The $\eta$ data are for water [23]. Their reciprocals and the ionisation data from Table 4 at each buffer concentration have hence been standardised to unity at 30°C. For SMZ the effects of increasing temperature upon ionisation and $1/\eta$ are generally comparable. For ST with a $pK_{a,2}$ value lower than for SMZ and closer to the buffer pH of 7, the effect of temperature on ionisation is less and the

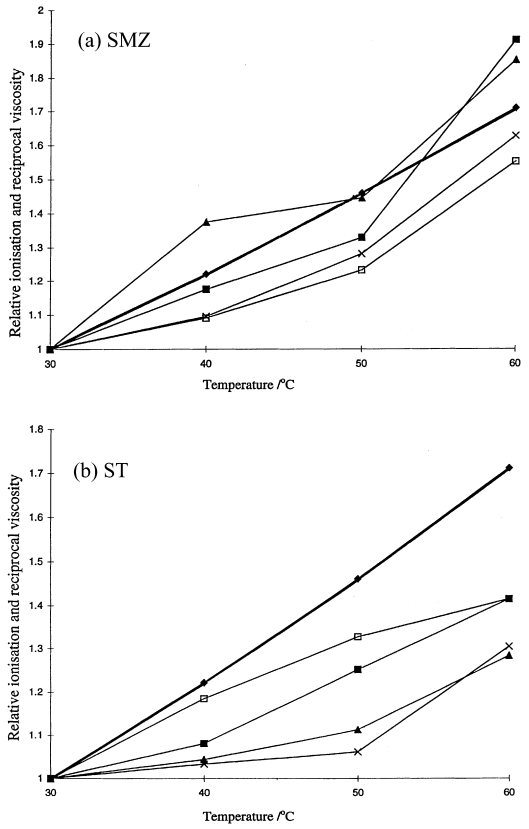


Fig. 3. Relative variations in reciprocal viscosity (♦, heavier line) and ionization versus the temperature. Reciprocal viscosity is referred to the reference value at 30°C: $(1/\eta_t)/(1/\eta_{30})$. Ionisation is referred the value at 30°C and the same ionic strength: $\alpha(t,I)/\alpha(30,I)$. (a) SMZ and (b) ST. Legend: (■) 101 m*M* buffer, (▲) 138 m*M*, (×) 174 m*M*, (□) 210 m*M* buffer.

variation in $1/\eta$ is dominant. For SMI and PSAC virtually complete ionisation means that the effect of temperature is purely via $1/\eta$.

### *4.4. Estimations of mean buffer temperatures due to Joule heating*

In Fig. 2 the solid curves drawn through the data are approximate curves of best fit that have been drawn by hand to the experimental data. The dashed lines are estimates of the likely $\mu_{ep}$ versus $1/\sqrt{I}$ behaviour at low buffer concentrations (high $1/\sqrt{I}$) extrapolated to high buffer concentrations (low $1/\sqrt{I}$). The deviation of the solid curve from the dashed line may therefore be attributed to the effects

of Joule heating and the underlying salt effects upon ionisation, where appropriate. Given the scatter and pattern of the experimental data, the exact shape and positioning of the curves of best fit are uncertain. However, over the region of deviation of the solid curve from the dashed line, it is at the highest buffer concentration (210 m*M*, lowest $1/\sqrt{I}$) where the positions of the curves of best fit appear to be in least doubt. Furthermore, the magnitudes of the deviations are greatest and may thus be most accurately measured.

Column 2 of Table 5 gives these deviations as percentages of the extrapolated, expected values of $\mu_{ep}$. The relative magnitudes are substantially as expected, with the fully ionised SMI and PSAC (that may only be affected via $1/\eta$) showing equal deviations that are far smaller than for the partially ionised analytes. The significantly larger percentage deviations for the other three SFA indicate substantial increases in ionisation in addition to decreased viscosity. In the case of SMZ, this is exactly as predicted from the partition and ionisation experiments. For ST it is less clear, since the salt effect upon ionisation (at fixed temperature) is negative, with the result that the increase in $\mu_{ep}$ due to increasing $1/\eta$ (with increasing temperature) may either be enhanced or diminished by the accompanying salt effect, depending upon the final temperature. (See line 1, then column 5 of ST part of Table 4).

The percentage deviation in $\mu_{ep}$ for SST would be expected to be a fraction of that of ST. Since the succinyl group will be fully ionised at pH 7, relative to ST the change in *Z* will be of the order of $0.4/1.4 \approx 0.3$. This estimate, however, is only be a rough approximation since the acid and base conjugates of SST are mono- and divalent ions respectively and thus will be subject to differing relative nonideal interactions in the electrolyte solutions. About 0.5 is the relativity observed.

Fig. 4 shows the cumulative effects of ionisation and temperature upon $\mu_{ep}$ for each of SMZ and ST. The calculation was:

$$\frac{1/\eta_t}{1/\eta_{30}} \cdot \frac{\alpha(t,I)}{\alpha(30,0)} \quad (9)$$

where *T* is the temperature. The reference values of $\alpha$ at 30°C were obtained by extrapolation to zero ionic strength. This yielded values of 0.300 for SMZ (compared with $\alpha = 0.285$ at 25°C from $pK_{a,2} = 7.4$) and 0.416 for ST (compared with $\alpha = 0.387$ at 25°C from $pK_{a,2} = 7.2$).

From Table 5, $\mu_{ep}$ for SMZ in 210 m*M* buffer is 168% of the value extrapolated from dilute buffers at 30°C. From Fig. 4, from the combined effects of

Table 5
Observed electrophoretic mobilities expressed as a percentage of the extrapolated dilute solution behavior

| | Buffer concentration (m*M*) | | | |
|---|---|---|---|---|
| | 210 | 174 | 138 | 101 |
| SMZ | 168 | | | |
| ST | 156 | | | |
| SMI | 117 | 110 | 109 | 107 |
| SST | 130 | | | |
| PSAC | 116 | 111 | 109 | 107 |

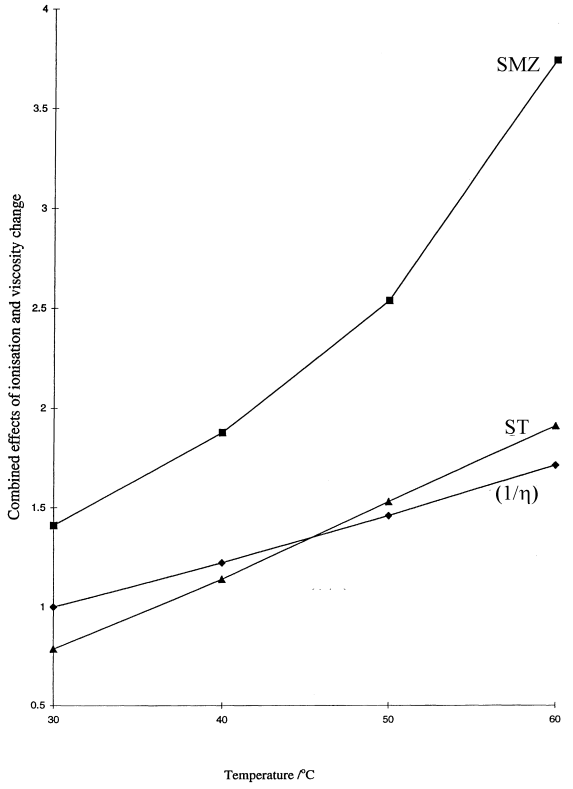


Fig. 4. Calculated net relative variations in the electrophoretic mobilities due to the ionisation of SMZ and ST and the reciprocal of the viscosity versus the temperature. The calculation is given in Eq. (8). The line marked $1/\eta$ is relative to 30°C and is the same line as plotted in Fig. 3.

ionisation and viscosity changes for SMZ at 1.68, this yields a mean internal temperature of 36.3°C. Since SMI and PSAC are virtually fully ionised at pH 7 under all circumstances, the 117 and 116% values, respectively, in 210 m*M* buffer are due to the viscosity variation alone. From the $1/\eta$ plot at 1.17 and 1.16, the internal capillary temperature is thus estimated to be 37.5 and 37.0°C, respectively.

Given the lesser scatter of the electrophoretic mobility data for SMI and PSAC, the curves of best fit for these analytes in Fig. 2 have been used to obtain the data in Table 5 and estimate the internal capillary temperatures at the other, higher buffer concentrations. In 174 m*M* buffer, the estimated temperatures are 34.3 and 34.7°C, respectively, in 138 m*M* buffer 33.9°C for both analytes and in 101 m*M* buffer, 33.0°C in each case. Fig. 5 is a plot of these estimated internal temperatures. As would be expected, decreasing buffer concentrations and thus higher solution resistances lead to lower power dissipation (at fixed voltage) and less internal heating.

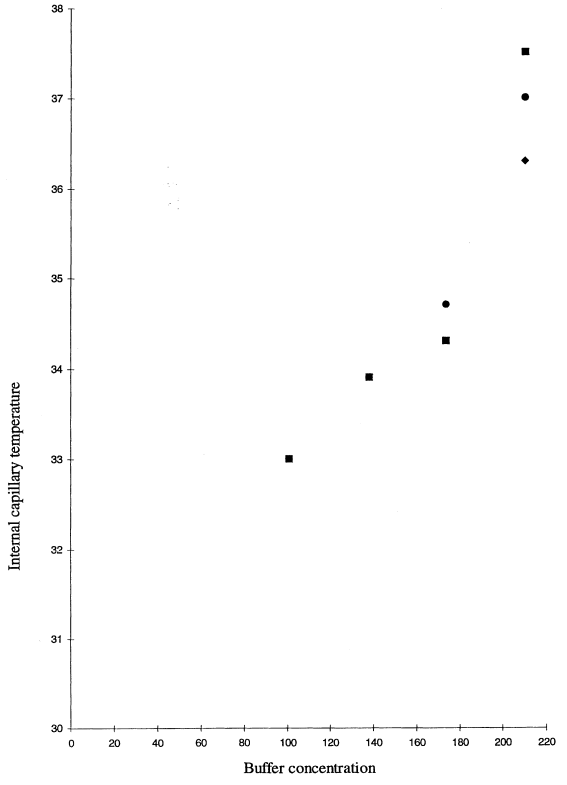


Fig. 5. Mean internal capillary temperatures estimated from electrophoretic mobility deviations from dilute solution behaviour for SFA analytes plotted as a function of the buffer concentration (m*M*). Legend: (♦) SMZ, (■) SMI, (●) PSAC.

### *4.5. Comparison of the calculated Joule heating with alternative estimates*

Several studies have estimated internal temperature rises from experimentally observed data mediated by known physical relationships [1,24,25]. However, it is difficult to make direct comparisons since each case is different in respect to capillary dimensions, thermostatting or absence of it and/or the specific buffers and their concentrations. In the case of the comprehensive examination of CZE dispersive processes by Foret et al. [24], a preliminary indication of the reasonableness of the above estimates may be obtained from a rule of thumb independent of these experimental variables. A mobility increase of 2.4% per K change in the internal capillary temperature, can be used as a quick check of our conversion of the Table 5 data for the fully ionised analytes to internal capillary temperatures. For SMI a 17% change would thus correspond to a temperature rise of 7.1 K, compared with our estimate of 7.5 K in 210 m*M* buffer. As the data in Fig. 5 is vaguely linear, a similar correspondence would be obtained for the other data as well.

Knox and McCormack [1] have devised three methods of calculating internal temperatures. We have applied each of these to data collected at the voltages contained in Table 2. The bases for the calculations and the estimates of the internal temperatures for the 210 m*M* buffer where maximal Joule heating would occur are: (a) increase in electroosmotic velocity ($v_{eo}$) with applied field strength ($E$), 57.6°C (using Eq. (6) [1]) or 58.6°C (using tabulated data [23])*; (b) increase in current ($I$), 58.5°C*; (c) increase in electrophoretic mobility of samples $(v_s - v_{eo})/E$, for SMI (fully ionised), 59.7°C*. As was the case with the original calculations of Knox and McCormack, excellent agreement is obtained between the three methods. The authors state that these three methods are independent. This is certainly so, inasmuch as three different measurable variables are utilised. But each of these variables is directly related to rates of ionic migration as

a function of the applied field strength and is mediated by the viscosity. And furthermore, these dependences are used in the estimations. Plots of ($v_{eo}$, $I$, or, $v_s - v_{eo})/E$ versus $E$ are extrapolated to zero field strength, the known viscosity at the operational CZE temperature is used to evaluate a constant of proportionality in the absence of Joule heating and this constant is then used at higher field strengths to determine the altered viscosity and thus the modified temperature. Hence, reasonable agreement might not be surprising.

Our plots are very similar to those of Knox and McCormack [1]. However, with an operational CZE temperature of 30°C, the estimated internal heating of 28–29°C is approximately four times the value we determined from our experiments, which was very close to that arrived at on the basis of the rule of thumb of Foret et al. [24]. The reasons for this large discrepancy are unclear. The methods of Knox and McCormack depend upon the temperature independence of a constant of proportionality in each case. The authors have provided some background to this and we are unable to comment further. The other obvious presumption of their methods is that the temperature dependence of the viscosity of buffer solutions — in our case moderately concentrated at 210 m$M$ with respect to phosphate — is the same as for water. Although we do not have data with which to shed light on this area, we feel that this could well be a source of significant error. This would of course also affect our estimates.

In an attempt to resolve these differences, we have looked at the effect of generated power upon column temperature. In their experimentation, Knox and McCormack used a variety of capillaries and buffers (six combinations, Table 1, [1]), each over a range of power outputs. For all of these variations, the averages of the estimated internal temperatures from methods (a) to (c) were plotted against the generated power (Figure 10, [1]). The data fall into two bands, according to the outside diameter of the capillary (O.D., 375 and 250 μm), are apparently linear at lower power, but deviate downwards at higher power outputs. The upper set of data points (for the lower O.D., 250 μm capillaries) have little scatter so that a curve of best fit may be confidentially drawn to them. This provides a first approximation to the internal heating (or excess heat, $\theta$) of 25°C for our most extreme conditions of experimentation (210 m$M$ electrolyte, $V$=18 kV, $L$=67.3 cm, $E$=26.7 kV m$^{-1}$, $I$=149 μA) with EI=1.49 W m$^{-1}$. However, this must be corrected for the difference in O.D. for our experiments (220 μm). With the use of Equation 18 of [1], $\theta$ becomes 26°C. It is also obvious from the Knox and McCormack data (Figure 10, [1], for the 375 μm O.D. capillary) that heat dissipation is more efficient from more highly concentrated buffers. As their sets of data for both O.D.s indicate that the I.D. has little practical effect, an increase from 0.02 – 0.05 $M$ buffer clearly has no effect whilst a further increase to 0.083 $M$ decreases $\theta$ to 23°C at EI=1.49 W m$^{-1}$. If this acceleration of the effect is correct, then a considerably larger downward correction would be required for our 0.210 $M$ buffer. Conservatively then (doubling the previous downward correction), we guesstimate that $\theta$ is probably $<$17°C.

However, all of the Knox and McCormack data [1] is predicated upon their experimental conditions, one of which was cooling by natural convection only. In our forced cooling system, heat dissipation will be far more efficient. The work of Lui et al. [9] provides some guidance here. At a power output around 2 W m$^{-1}$, $\theta$ dropped from about 30 to 18°C when free-air cooling was replaced by forced air cooling. Applying this fractional decrease, $\theta \approx 10$°C — and this appears to be an underestimate of the likely effect of forced air cooling. From the calculated equivalent heat transfer coefficient, Lui et al. estimate that their heat removal system lies only midway between stagnant air and the efficiency expected by forced air cooling. Our final conclusion then, is that if the methods of calculation of internal heating of Knox and McCormack [1] are correct for their system, appropriate correction leads to an expectation of $\theta < 10$°C and compatible with our estimate of about 7°C.

The data of Lui et al. [9] provides another reference point in itself. The 18°C rise in internal temperature observed with the application of 1.7 W m$^{-1}$ would be equivalent to 15.8°C in our case of 1.49 W m$^{-1}$. Again, as the heat removal system of Lui et al. was considerably less efficient than expected of forced air cooling, a value of $\theta < 10$°C might be expected. Again the result is compatible with our findings and incompatible with the values of 28–29°C obtained by the methods of estimation due to Knox and McCormack [1].

The ST results are at odds with the other three analytes for which all of the relevant data is known. From Fig. 4 it is clear that much higher internal capillary temperatures would be predicted. For example, at 210 m*M* buffer, 51.8°C is obtained. The reasons for this are not clear. Unless the internal temperature of the capillary is large, the two sets of experimental data upon which the estimate depends appear to be in conflict. The large deviation of the measured $\mu_{ep}$ from the extrapolated behaviour at low buffer concentrations implies a large increase in ionisation with increasing buffer concentrations. At low temperatures (30–40°C), the ionisation data from the partition experiments shows the opposite. Alternatively, the ionisation data implies a proportionately more negative gradient for ST than the other analytes. This is clearly not the case. It difficult to see how the data for this analyte could be correct and the data for SMZ, SMI and PSAC all incorrect, especially when these three are internally consistent and give rise to internal heating of an apparently sensible magnitude.

## 5. Conclusions

Increasing the salt concentration in a buffer has multiple effects.

(a) For analytes migrating away from the detector and in the opposite direction to the EOF, migration times diverge and separation is enhanced.

(b) Strongly ionised analytes will not experience significant changes in ionisation, but weakly ionised acids and bases can exhibit differential changes. This provides a mechanism for selective adjustment of mobilities and the potential for the resolution of otherwise comigrating analytes.

(c) If high voltages are used to minimise analysis times, the Joule heating produced will enhance the degree of ionisation through an increase in the equilibrium constant for ionisation. Hence the selectivity may be enhanced, since, the smaller the degree of ionisation of an analyte in water at the thermostated temperature, the larger is the potential change in the electrophoretic mobility.

(d) A simple procedure has been described for the estimation of average internal capillary temperatures. For a fully ionised analyte, extrapolation of measured electrophoretic mobilities from low $1/\sqrt{I}$ to higher values, subtraction of this from the observed $\mu_{ep}$ and conversion of that percentage change through the same percentage change in $1/\eta$ provides the temperature.

(e) Joule heating has been estimated to give temperature rises ranging from 3 to 8 K for phosphate buffers of 100 to 210 m*M*, respectively.

## References

[1] J.H. Knox, K.A. McCormack, Chromatographia 38 (1994) 207–214.
[2] A. Vinther, H. Søeberg, J. Chromatogr. 559 (1991) 27–42.
[3] J.W. Jorgenson, K.D. Lukacs, J. Chromatogr. 218 (1981) 209–216.
[4] M.S. Bello, P.G. Righetti, J. Chromatogr. 606 (1992) 95–102.
[5] M.S. Bello, P.G. Righetti, J. Chromatogr. 606 (1992) 103–111.
[6] A.E. Jones, E. Grushka, J. Chromatogr. 466 (1989) 219–225.
[7] J.H. Knox, Chromatographia 26 (1988) 329–337.
[8] E. Grushka, R.M. McCormick, J.J. Kirkland, Anal. Chem. 61 (1989) 241–246.
[9] K.-L.K. Lui, K.L. Davis, M.D. Morris, Anal. Chem. 66 (1994) 3744–3750.
[10] L. Yu, T.H. Seals, J.M. Davis, Anal. Chem. 68 (1996) 4270–4280.
[11] H.J. Issaq, I.Z. Atamna, G.M. Muschik, G.M. Janini, Chromatographia 32 (1991) 155–161.
[12] I.Z. Atamna, H.J. Issaq, G.M. Muschik, G.M. Janini, J. Chromatogr. 588 (1991) 315–320.
[13] J. Cao, R.F. Cross, J. Chromatogr. A 695 (1995) 297–308.
[14] R.F. Cross, J. Cao, in: D. Dundas, B. Salter-Duke (Editors), Proceedings 13th Australian Symp. Anal. Chem., Royal Australian Chem. Institute, Darwin, 1995, AO18/1-4.
[15] A. Leo, C. Hansch, D. Elkins, Chem. Rev. 71 (1971) 525–616.
[16] T.D. Rotsch, R.J. Sydor, D.J. Pietrzyk, J. Chromatogr. Sci. 17 (1979) 339–343.
[17] Model 270A User's Manual, Applied Biosystems, Santa Clara, CA, 1989.
[18] R.A. Robinson, R.H. Stokes, Electrolyte Solutions, Butterworths, London, 2nd ed., 1959, Ch. 15.
[19] R.F. Cross, Ph.D. Thesis, University of Melbourne, 1972.
[20] W.F. McDevit, F.A. Long, Chem. Rev. 51 (1952) 119–169.
[21] R.F. Cross, P.T. McTigue, J. Phys. Chem. 80 (1976) 814–821.
[22] R.F. Cross, J. Cao, J. Chromatogr. A 786 (1997) 171–180.
[23] CRC Handbook of Chemistry and Physics, R.C. Weast (Editor), CRC Press, Boca Raton, FL, 60th ed., 1980, p. F–49.
[24] F. Foret, M. Deml, P. Bocek, J. Chromatogr. 452 (1988) 601–613.
[25] S. Terabe, K. Otsuka, T. Ando, Anal. Chem. 57 (1985) 834–841.